Phase-sensitive stimulated Raman adiabatic passage in dipolar extended lambda systems

Christoph A. Marx[a] and Werner Jakubetz[b]
Institut für Theoretische Chemie, Universität Wien, Währingerstraße 17, 1090 Wien, Austria

(Received 27 October 2006; accepted 8 November 2006; published online 19 December 2006)

The authors investigate the possible phase-sensitive behavior of (multiphoton) stimulated Raman adiabatic passage population transfer in extended lambda systems, if more than one state of an anharmonic progression of target levels is accessible in transitions of different photonicities. They use a minimal model four-level system (4LS) with one initial state separated from two target states by an apex state. The parameters of the 4LS are adapted from the bend states of the HCN-HNC system. Using a dressed-state analysis within the rotating wave approximation (RWA), the authors identify phase-dependent diabatic transitions between the two dressed states contributing to the state vector as the mechanism leading to phase-sensitive target populations. The essential features giving rise to the phase dependence are found to be different (non-zero-) diagonal elements of the dipole matrix, i.e., permanent dipole moments, and the presence of a direct two-photon overtone coupling between the apex state and the lower target state which formally enters the RWA Hamiltonian upon inclusion of permanent dipole moments. Among the parameters controlling the extent of the effect are the anharmonic properties of the target progression and the absolute values of the field frequencies, so that in view of the requirement to tune the driving fields into the vicinity of resonance, details of the level structure are of importance. A comparative numerical study executed without invoking RWA shows that qualitatively there are similar trends in the appearance of phase sensitivity, although the effects are considerably more pronounced in the full treatment. In the full treatment the authors also explore off-resonance conditions and discuss the signatures of phase sensitivity in the target populations. © *2006 American Institute of Physics*. [DOI: 10.1063/1.2403880]

I. INTRODUCTION

Following its development in the early 1990s, the technique of stimulated Raman adiabatic passage[1,2] (STIRAP) has been widely used in various branches of physical science such as atom and quantum optics, cavity quantum electrodynamics, and chemical reaction dynamics. Originally designed as a two-pulse strategy for three-level Λ systems making use of the counterintuitively overlapping pump and Stokes pulse,[3] its extension to more complex systems and to applications using several pulses has been pushed forward over the last decade.[4–6] It has also been popular with experimentalists, because of its simple practical implementation when compared to more traditional transport schemes such as stimulated emission pumping.[7] This relates to the fact that with STIRAP the necessity of thoroughly controlling the details of the pulses, in particular, of their area, can be overcome.

In this connection it has been widely accepted that most coherent control processes using STIRAP-like dynamics are independent of the relative phase among the control fields.[8] Although a few exceptions have been found, where phase dependencies become of importance,[8,9] these systems are rather special and complex in structure.

Interestingly thus, when studying the application of a multiphoton extension of STIRAP to the isomerization process of HCN→HNC,[10] it was noted that there exists phase-sensitive behavior with respect to the final population of the target states. This effect was detected in a specific region in frequency space, spanned by the pump (ω_P) and Stokes (ω_S) frequencies, which was centered along a line corresponding to simple *commensurable frequencies* of the form $\omega_P:\omega_S = 3:2$.

We take this observation as a starting point for our work and examine the conditions that lead to this interesting phenomenon. As a model system for these investigations we use the most simple suitable subsystem of the HCN/HNC system reported in Ref. 10, consisting of only four levels. It comprises an initial state being separated from two target states by an intermediate state, the apex state of the extended Λ system. Near its respective resonance conditions, this system permits population transfer from the initial state either to the upper target state in a (1+1)-STIRAP process (one-photon-pump+one-photon Stokes transition) or to the lower target state in a (1+2)-STIRAP process (one-photon-pump +two-photon Stokes transition). If these transfer processes occur in parallel, phase-sensitive behavior may appear. Based on an analytical analysis of the dynamics, we try to explore the conditions for this phase dependence. In particular, the role of simple commensurable frequencies, as suggested previously,[10] is examined.

We organize the paper as follows: After a short introduc-

[a]Electronic mail: cmarx@uci.edu
[b]Electronic mail: werner.jakubetz@univie.ac.at

tion to the problem in Sec. II, we turn to its discussion within the rotating wave approximation (RWA) in Sec. III. This discussion is divided into first analyzing the dynamics of the system in Sec. III A, and subsequently applying these insights to the question of the influence of the relative phase on the outcome of the transport process in Sec. III B. Aiming at analytical results, we constrain these investigations to on-resonance conditions for the (1+1) process. In Sec. IV the implications drawn from this treatment within the framework of the RWA are compared with the results from a full numerical study of the problem. The direct comparison for the (1+1)-on-resonance conditions is given in Sec. IV A, while in Sec. IV B we look separately at the previously detected elements of phase sensitivity. Furthermore in Sec. IV C, extending the investigations to off-resonant frequencies, we explore the signatures of phase sensitivity in a wider context and address the question of the influence of phase-sensitive behavior on the robustness of STIRAP. Finally, Sec. V provides a summary of the results and of our conclusions.

We note that in our presentation we make extensive use of a.u. This implies $\hbar=1$, which we omit from all equations, as well as the numerical equivalence of circular frequency and energy, which we use interchangeably. The relevant conversion factors are[11] 1 a.u. of field strength $=514.225\ \mathrm{GV\,m^{-1}}$, 1 a.u. of dipole moment $=2.541\,76\ \mathrm{D}=8.478\,41\times10^{-30}\ \mathrm{C\,m}$, 1 a.u. of energy $=1$ hartree $=27.2116\ \mathrm{eV}=4.359\,81\times10^{-18}\ \mathrm{J}$, and 1 a.u. of circular frequency $=6.579\,68\times10^{15}$ Hz, corresponding to a wave number of $219\,474\ \mathrm{cm^{-1}}$.

II. DEFINITION OF THE PROBLEM

A. Basic definitions and equations

We consider a four-level system (4LS) in an extended Λ configuration, interacting with two temporally overlapping laser pulses: the pump (P) and Stokes (S) pulses, which are adjusted to the frequencies of the underlying Λ system. This interaction is treated semiclassically and we assume the dipole approximation to be valid. The dynamics of the system are governed by the time-dependent Schrödinger equation

$$i|\dot{\psi}\rangle = \hat{H}(t)|\psi\rangle, \qquad |\psi(t_0)\rangle =: |\psi_0\rangle, \tag{1}$$

with a Hamiltonian given by

$$\hat{H}(t) = \hat{H}_0 + \hat{V}(t), \qquad \hat{V}(t) = -\hat{\mu}\cdot\mathbf{E}(t). \tag{2}$$

Here $\hat{H}_0$ is the Hamiltonian of the bare system and $\hat{V}(t)$ accounts for the interaction with the laser fields within the dipole approximation.

The component of the field acting in the direction of the dipole moment is assumed to be of the form

$$E(t) := E_P\cos(\omega_P t+\delta) + E_S\cos(\omega_S t), \tag{3}$$

where δ refers to the relative phase among the two pulses at time zero. Without loss of generality we have incorporated this phase in the term of the pump pulse. We consider the limiting case $t_0\to-\infty$ in Eq. (1). Consequently, the "end" of the interaction then corresponds to $t\to+\infty$.

As common in the description of spectroscopic processes, we use the eigenstates of $\hat{H}_0$, $\{|j_0\rangle : 1\leqslant j\leqslant 4\}$, as a basis of the Hilbert space, and solve for the solutions of the initial value problem Eq. (1) in an equivalent matrix representation with respect to the chosen basis set,

$$i\dot{\mathbf{c}} = \mathbf{H}(t)\mathbf{c}, \qquad \mathbf{c}(t_0) =: \mathbf{c}_0. \tag{4}$$

We refer to this basis as the *spectroscopic basis*, and we indicate its elements by the index "0." The corresponding energy eigenvalues are denoted by ω_j, $1\leqslant j\leqslant 4$.

STIRAP being an adiabatic technique,[1,12,13] it is favorable to work in the interaction representation (IR) and to subsequently apply the RWA.[14,15] Following the adiabatic theorem,[16] the dynamics of the system is then most naturally displayed by expanding the state vector in the elements of the *adiabatic basis* (or basis of *dressed states*), $\{|j(t)\rangle : 1\leqslant j\leqslant 4\}$.

Within the adiabatic approximation,[16] searching for the solution of the initial value problem Eq. (4) is replaced by an eigenvalue problem for the time-dependent RWA-Hamiltonian matrix. For the special case of a nondegenerate system, the following *necessary* local condition for the validity of the adiabatic approximation may be established:[2,16]

$$|\langle\dot{k}(t)|l(t)\rangle| \ll |\epsilon_k(t)-\epsilon_l(t)|, \quad k\neq l\in\{1,4\}, \tag{5}$$

which leads to a pictorial way of obtaining insight into possible diabatic transitions during the evolution of the state vector. In the inequality Eq. (5), $\{\epsilon_j(t) : 1\leqslant j\leqslant 4\}$ refers to the set of nondegenerate eigenvalues of $\hat{H}(t)$, which in analogy to the corresponding basis of eigenstates are termed *dressed energies*.

As we are interested in the dynamics of our 4LS as a basis for understanding phase dependences with respect to the final populations, we look for the existence of a *transport state*[6] (or *transfer state*), $|\psi_T\rangle$, generally defined as

$$|\psi_T\rangle \xrightarrow{t\to-\infty} |i\rangle, \tag{6}$$

$$|\psi_T\rangle \xrightarrow{t\to+\infty} |f\rangle, \tag{7}$$

with $|i\rangle$ and $|f\rangle$ referring to the initial and final states, respectively.

B. Description of the system

A sketch of the extended-lambda 4LS is given in Fig. 1. As pointed out in Sec. I, it is derived from the HCN/HNC system used in a previous study of the application of STIRAP to molecular isomerization.[10] It consists of the two states $|3_0\rangle$ and $|4_0\rangle$, separated from the initial state $|1_0\rangle$ by an intermediate state $|2_0\rangle$. Since the objective is to understand phase-dependent final populations of the spectroscopic states $|3_0\rangle$ and $|4_0\rangle$, both are considered as target states.

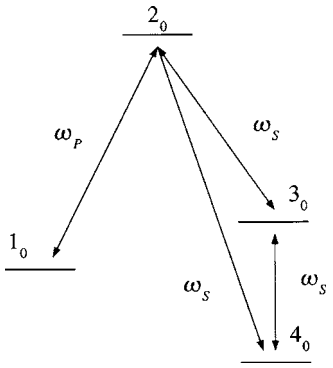

FIG. 1. Schematic representation of the model four-level system with states $|1_0\rangle$–$|4_0\rangle$. The associated energy levels are denoted ω_1–ω_4. By ω_P and ω_S we denote, respectively, the carrier frequencies of the pump pulse, which couples the initial state $|1_0\rangle$ to the intermediate (apex) state $|2_0\rangle$, and the Stokes pulse, which couples the states of the progression $|2_0\rangle$, $|3_0\rangle$, $|4_0\rangle$. States $|3_0\rangle$ and $|4_0\rangle$ are the target states of possibly competing (1+1)- and (1+2)-STIRAP transport processes. For simplicity, in the RWA treatment we consider only the (1+1)-on-resonance case where ω_P and ω_S are in turn tuned to the zero-order transition frequencies of $|1_0\rangle \leftrightarrow |2_0\rangle$ and $|2_0\rangle \leftrightarrow |3_0\rangle$. In the RWA treatment, the direct overtone coupling between $|2_0\rangle$ and $|4_0\rangle$ becomes relevant only upon inclusion of permanent dipole moments. Variation of the pump:Stokes frequency ratio and the anharmonicity are achieved independently by adjusting, respectively, ω_1 and ω_4 while leaving the remaining levels unchanged.

The levels are assumed to be sequentially coupled; however, there exists an additional two-photon coupling $|2_0\rangle \leftrightarrow |4_0\rangle$, which will turn out to be crucial for phase-dependent dynamics. In addition, the spectroscopic states also have nonzero permanent dipole moments μ_{jj}, whose effects on the system's temporal evolution will have to be considered in deeper detail.

For establishing STIRAP-like population transport, we neglect all tunneling couplings, so that

$$\mu_{13} = \mu_{14} := 0. \tag{8}$$

Furthermore, in order to implement the common assumption of level pairs coupled by only one of the two laser fields when invoking the RWA, which we refer to as the *coupling approximation*, the system is considered to be derived from one with harmonic energy level progression on the target side $\{|2_0\rangle, |3_0\rangle, |4_0\rangle\}$. The couplings among these states are associated solely with the Stokes pulse. For later use, we define the detuning Δ_h,

$$\Delta_h := \omega_3 - \omega_4 - \omega_S, \tag{9}$$

which for (1+1)-on-resonance conditions can be rewritten as

$$\Delta_h := (\omega_3 - \omega_4) - (\omega_2 - \omega_3). \tag{10}$$

In view of Eq. (10), we denote Δ_h the "anharmonicity." For the characterization of the anharmonic effects it is appropriate to use a system-independent relative measure, for which we introduce the anharmonicity ratio f_h, defined as

$$f_h := 1 + \frac{\Delta_h}{\omega_2 - \omega_3} = 1 + \frac{\Delta_h}{\omega_S}. \tag{11}$$

Accordingly, a harmonic target progression has $f_h = 1$.

As for our objective to find analytical expressions within the RWA for the conditions under which phase-dependent behavior occurs, we concentrate on the (1+1)-on-resonance case so that $\omega_P = \omega_2 - \omega_1$ and $\omega_S = \omega_2 - \omega_3$. In order to examine the role of commensurable frequencies, we will vary the pump:Stokes ratio f_{PS},

$$f_{\mathrm{PS}} := \frac{\omega_P}{\omega_S} = \frac{\omega_2 - \omega_3}{\omega_2 - \omega_1}, \tag{12}$$

where the second equality again holds for (1+1)-on-resonance conditions. Since phase-sensitive behavior was first detected for $f_{\mathrm{PS}} \approx 1.5$, we will use this special case (the "3:2-4LS") as an example for illustrating the conclusions drawn within the RWA treatment and as a starting point for practical calculations. Keeping now levels $|2_0\rangle$ and $|3_0\rangle$ fixed, we are able to independently vary the parameters f_h and f_{PS} by adjusting, respectively, ω_4 and ω_1.

The elements of the dipole matrix are also adapted from Ref. 10. Tables I and II summarize the energies (referring to the 3:2-4LS) and elements of the dipole matrix that are used in the present paper. If not specified explicitly, the parameters are assumed to be chosen as indicated here.

In our numerical calculations with the full Hamiltonian, we use a pair of Gaussian pulses with equal envelope. The parameters characterizing these pulses,

$$E_\alpha(t) = E_{0,\alpha} \exp\left(-\frac{\ln 2(t - t_\alpha)^2}{\tau_{H,\alpha}}\right), \tag{13}$$

are summarized in Table III. If not explicitly indicated, we take this as our standard pulse setting, which we have also used in the calculations illustrating the developments of the RWA treatment. The corresponding carrier frequencies, ω_α, are adjusted to meet the (1+1)-on-resonance conditions given in Eq. (17). To numerically deal with the temporally

TABLE I. Energy spectrum of the 3: 2-4LS.

State	Energy (a.u.)[a]
$\|4_0\rangle$	−0.006 983 47
$\|1_0\rangle$	−0.005 087 60
$\|3_0\rangle$	−0.003 391 73
$\|2_0\rangle$	0.0

[a]Adapted from Ref. 21.

TABLE II. Dipole matrix elements for the model 4-LS.

(j,k)	μ_{jk} (a.u.)[a]
(1,1)	−0.713 134
(2,1)	−0.200 000
(2,2)	−0.133 002
(3,1)	0.0
(3,2)	−0.200 000
(3,3)	0.440 670
(4,1)	0.0
(4,2)	−0.066 6667
(4,3)	0.300 000
(4,4)	0.471 846

[a]From Ref. 22.

TABLE III. Standard pulse parameters.

	$E_{0,\alpha}$ (a.u.)	t_α (ps)[a,b]	$\tau_{H,\alpha}$ (ps)
Stokes (S)	0.0045	11.0	4.0
Pump (P)	0.0045	18.3	4.0

[a]The entries relate to the total integration time of 30 ps.
[b]Delay adjusted to optimize population transfer in the underlying three-level Λ system, $\{|1_0\rangle,|2_0\rangle,|3_0\rangle\}$.

infinitely extended field, we cut it off when there occur no changes in the populations for the chosen numerical precision. Applied to the pulse parameters of Table III, this gives rise to an overall intergration time of 30 ps.

III. TREATMENT WITHIN THE ROTATING WAVE APPROXIMATION (RWA)

A. Dynamics in the extended Λ system

Before being able to discuss the role of the relative phase on the final populations of the target states, a thorough understanding of the underlying dynamics is required. We thus start our investigation with analyzing the system's "pure" dynamics, i.e., without making reference to δ. Since permanent dipole moments μ_{jj} will turn out to play a central role for phase-sensitive dynamics, we additionally split this discussion into two parts: *without* and *with* incorporating the effects of nonvanishing μ_{jj}. We start off with the former case.

1. Dressed states: The role of the anharmonicity

Defining the quantities

$$\Delta_P := \omega_2 - \omega_1 - \omega_P \tag{14}$$

and

$$\Delta_S := \omega_2 - \omega_3 - \omega_S, \tag{15}$$

which measure the frequency detunings with respect to the one-photon couplings $|1_0\rangle \leftrightarrow |2_0\rangle$ and $|2_0\rangle \leftrightarrow |3_0\rangle$, respectively, and setting $-\Delta_S$ as the zero of the energy scale, the RWA-Hamiltonian matrix of the system reads

$$\frac{1}{2}\begin{pmatrix} -2(\Delta_P-\Delta_S) & -\mu_{12}E_P & 0 & 0 \\ -\mu_{12}E_P & 2\Delta_S & -\mu_{23}E_S & 0 \\ 0 & -\mu_{23}E_S & 0 & -\mu_{34}E_S \\ 0 & 0 & -\mu_{34}E_S & -2\Delta_h \end{pmatrix}. \tag{16}$$

Inserting the resonance conditions, introduced in Sec. II B, for these one-photon detunings,

$$\Delta_P = \Delta_S = 0, \tag{17}$$

the characteristic equation with respect to the RWA-Hamiltonian matrix becomes

$$0 = 16\lambda^4 + 16\Delta_h\lambda^3 + 4\lambda^2\{-E_S^2(\mu_{23}^2+\mu_{34}^2) - \mu_{12}^2E_P^2\} + 4\Delta_h\lambda\{-\mu_{23}^2E_S^2 - \mu_{12}^2E_P^2\} + \mu_{12}^2\mu_{34}^2E_P^2E_S^2. \tag{18}$$

At this point we note that within the standard RWA, i.e., without including effects of permanent dipole moments, direct two-photon couplings (or n-photon couplings, in general) are excluded in principle at this level of theory.[14,17] This follows readily from the neglect of off-resonant terms when invoking the RWA.

Following Eq. (18), although considering the on-resonance case with respect to Δ_P and Δ_S, the characteristic polynomial still depends on one detuning, namely, Δ_h. We will thus have to distinguish among the two situations, $\Delta_h \neq 0$ and $\Delta_h = 0$. The former will be referred to as the *anharmonic*, the latter as the *harmonic* case.

In general, searching for the roots of the characteristic polynomial Eq. (18), which is of fourth order, will be a tedious process. In principle, closed form solutions to this particular eigenvalue problem are available,[18] but are rather unwieldy for further manipulation. However, as we are interested in the existence of a transport state, where the final state $|f\rangle$ in Eq. (6) can either be $|3_0\rangle$ or $|4_0\rangle$, it is sufficient to consider the beginning and the end of the process, respectively. This corresponds to the following two time intervals.

Initial period (IP): "Early times." Only the Stokes field interacts with the system, thus

$$E_S(t) \neq 0 \text{ and } E_P(t) = 0. \tag{19}$$

Final period (FP): "Late times." Only the pump field interacts with the system, thus

$$E_S(t) = 0 \text{ and } E_P(t) \neq 0. \tag{20}$$

Turning first to IP, the constant term in the characteristic polynomial vanishes, thus there exists an eigenvalue ϵ_1 with

$$\epsilon_1(t) = 0. \tag{21}$$

The roots of the remaining third-order polynomial

$$p(\lambda) := 16\lambda^3 + 16\Delta_h\lambda^2 - 4\lambda E_S^2(\mu_{23}^2+\mu_{34}^2) - 4\Delta_h\mu_{23}^2E_S^2 \tag{22}$$

depend on the choice of Δ_h in a crucial way. In the more general case of a nonvanishing constant term in Eq. (22), corresponding to $\Delta_h \neq 0$, there exists no other zero eigenvalue. Thus in this case the only eigenspace that *could* be related to a transport state is one dimensional,

$$\mathcal{V}_1 = \text{span}\{(1\ 0\ 0\ 0)^T\}. \tag{23}$$

For the special case where $\Delta_h = 0$, the eigenvalues can easily be calculated giving

$$\left.\begin{aligned} \epsilon_1(t) &= \epsilon_2(t) = 0 \\ \epsilon_3(t) &= \tfrac{1}{2}E_S\sqrt{\mu_{23}^2+\mu_{34}^2} \\ \epsilon_4(t) &= -\epsilon_3(t) \end{aligned}\right\} \quad \text{for } \Delta_h = 0. \tag{24}$$

Thus the harmonic system bears a two dimensional eigenspace $\mathcal{V}_{1,2}$ corresponding to a zero-valued dressed energy. $\mathcal{V}_{1,2}$ is given by

$$\mathcal{V}_{1,2} = \text{span}\left\{(1\ 0\ 0\ 0)^T; \frac{1}{N}(0\ -\mu_{34}\ 0\ \mu_{23})^T\right\}, \qquad N := \sqrt{\mu_{34}^2+\mu_{23}^2}. \tag{25}$$

For FP the characteristic equation may be rewritten in the form

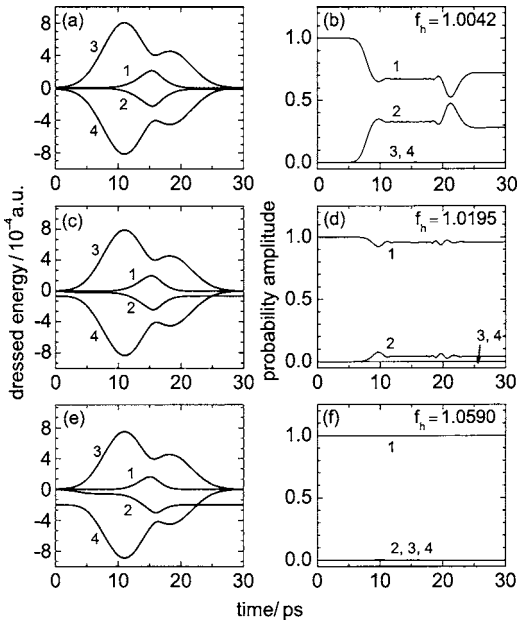

FIG. 2. Effects of the anharmonicity in the 3:2-4LS at (1+1)-on-resonance conditions. Panels (a), (c), and (e) show in turn the temporal behavior of the RWA dressed energies ϵ_j (as indicated) for the anharmonicity ratios f_h =1.0042, 1.0195, and 1.0834. Panels (b), (d), and (f) show the corresponding statistical weights $|c_j|^2$ of the dressed states $|j\rangle$ in the state vector $|\psi\rangle$ while the system evolves under a pulse pair in standard setting (Table III). Whereas in the quasiharmonic system (b) the dressed state $|2\rangle$ contributes strongly to the dynamics of the system, its contribution diminishes for increasing anharmonicity. In (f), the system evolution is completely described by the dressed state $|1\rangle$. The contributions of states $|3\rangle$ and $|4\rangle$ remain negligibly small in all cases.

$$0 = (2\Delta_h + 2\lambda) \cdot 2\lambda \cdot (4\lambda^2 - \mu_{12}^2 E_P^2). \tag{26}$$

The eigensystem for $\Delta_h \neq 0$ is then

$$\begin{aligned}
&\epsilon_1(t) = 0, \quad \mathcal{V}_1 = \mathrm{span}\{(0\ 0\ 1\ 0)^T\},\\
&\epsilon_2(t) = -\Delta_h, \quad \mathcal{V}_2 = \mathrm{span}\{(0\ 0\ 0\ 1)^T\},\\
&\epsilon_3(t) = \frac{1}{2}\mu_{12}E_P, \quad \mathcal{V}_3 = \mathrm{span}\left\{\frac{1}{\sqrt{2}}(1\ -1\ 0\ 0)^T\right\},\\
&\epsilon_4(t) = -\epsilon_3(t), \quad \mathcal{V}_4 = \mathrm{span}\left\{\frac{1}{\sqrt{2}}(1\ 1\ 0\ 0)^T\right\}.
\end{aligned} \tag{27}$$

Again for vanishing Δ_h, the eigenspace corresponding to a zero-valued dressed energy is two dimensional.

Thus, for the anharmonic system it is likely that a transport state exists, which links the initial state $|1_0\rangle$ with the target state $|3_0\rangle$. Strictly speaking, one would still have to show that the eigenspaces corresponding to zero eigenvalues on IP and FP are continuously connected. Instead of giving a rigorous proof, we will consider a numerical solution to the problem, which strongly suggests that such a continuous connection indeed exists. Figure 2 depicts the temporal behavior of the dressed energies for increasing Δ_h, starting with an almost harmonic system in (a), leading, via an intermediate case in (c), to a strongly anharmonic system in (e).

From the plots it can be inferred that the assumption of a dressed state with energy zero on both IP and FP is correct. Increasing f_h gradually lifts the quasidegeneracy. Recalling the necessary condition for adiabatic following in a system with distinct eigenvalues [Eq. (5)], one may also expect diabatic transitions to occur between the dressed states corresponding to ϵ_1 and ϵ_2, if Δ_h is sufficiently small. These transitions will become less pronounced as Δ_h increases. This behavior is displayed in panels (b), (d), and (f) of Fig. 2, where the RWA-state vector is projected onto the elements of a basis of instantenous eigenstates of the Hamiltonian matrix. The corresponding absolute squared value is equivalent to the statistical weight of the respective dressed state. The systems employed in panels (e) and (f) show no transitions anymore, hence they are completely described by state $|1\rangle$. According to RWA dynamics, it thus ends up completely in the spectroscopic state $|3_0\rangle$, with no contribution of $|4_0\rangle$.

From Fig. 2 it can also be concluded that diabatic transitions should occur when the dressed states "drift apart," which corresponds to the times when the system leaves IP and when it enters FP. On IP and FP themselves, as a consequence of zero couplings $\langle \dot{k}(t)|l(t)\rangle$, $k \neq l$, no transitions occur.

If there is a contribution of the dressed state $|2\rangle$, the system will end in a superposition of the spectroscopic states $|3_0\rangle$ (corresponding to $|1\rangle$) and $|4_0\rangle$ (corresponding to $|2\rangle$), see Eq. (27). For the anharmonic system, we may thus identify the mechanism for obtaining a superposition of the two target states $|3_0\rangle$ and $|4_0\rangle$ in the limiting case $t \to +\infty$, with diabatic transitions occurring among the transport state $|1(t)\rangle$ and the dressed state $|2(t)\rangle$.

So far, we have been mainly discussing the properties of the dynamics in the anharmonic case. This is for two reasons. First, since the harmonic case assumes Δ_h=0, it is a special case. In addition, there is still the subtlety of the twofold degeneracy of the zero eigenvalue $\epsilon_{1,2}$ on both IP and FP, which leads to certain difficulties with the correct choice of the elements of the adiabatic basis. In this respect it is essential to recall that whereas the eigenstates given in Eq. (25) are a possible basis for the invariant subspace $\mathcal{V}_{1,2}$ on IP, the adiabatic theorem demands a set of eigenvectors of the time-dependent Hamiltonian, which evolves *continuously* on the *entire* time interval the system interacts with the laser fields.[16] Only such eigenstates of $\mathbf{H}(t)$ are the correct choice for the adiabatic basis and hence enter the expression for the time-evolution operator as given by the adiabatic theorem.[16]

The properties of the adiabatic basis for a harmonic 4LS can be inferred from Ref. 6. Applied to the system discussed here, it is shown that the initial state $|1_0\rangle$ is *not* an element of the adiabatic basis at the beginning of the interaction $t \to -\infty$, but rather a superposition of the dressed states $|1\rangle$ and $|2\rangle$ with equal statistical weights,

$$|1^{(-\infty)}\rangle = \tfrac{1}{\sqrt{2}}(1 - \sin\vartheta_S^{(-\infty)} 0 \cos\vartheta_S^{(-\infty)})^T, \tag{28}$$

$$|2^{(-\infty)}\rangle = \tfrac{1}{\sqrt{2}}(1 \sin\vartheta_S^{(-\infty)} 0 - \cos\vartheta_S^{(-\infty)})^T, \tag{29}$$

$$\text{where } \tan\vartheta_S^{(-\infty)} = \frac{\mu_{23}}{\mu_{34}}, \tag{30}$$

$$\text{thus } |\psi^{(-\infty)}\rangle = |1_0\rangle = \tfrac{1}{\sqrt{2}}\{|1^{(-\infty)}\rangle + |2^{(-\infty)}\rangle\}. \tag{31}$$

Hence, there exists *no* transport state in accordance with the definition introduced in Eq. (6) for the harmonic system. Assuming the system evolves adiabatically, the state vector for $t \to +\infty$ reads

$$|\psi^{(+\infty)}\rangle = \frac{1}{\sqrt{2}}\{e^{-i\gamma_1}|1^{(-\infty)}\rangle + e^{-i\gamma_2}|2^{(+\infty)}\rangle\},$$
$$\gamma_j := \int_{-\infty}^{+\infty} \epsilon_j(t)dt, \quad j \in 1,2, \tag{32}$$

which by insertion of the expressions for the respective elements of the adiabatic basis on FP given in Ref. 6,

$$|1^{(+\infty)}\rangle = \frac{1}{\sqrt{2}}(0\ 0\ -1\ 1)^T, \quad |2^{(+\infty)}\rangle = \frac{1}{\sqrt{2}}(0\ 0\ 1\ 1)^T \tag{33}$$

leads to the final populations $|c_j^{(+\infty)}|^2$ of the spectroscopic states $|j_0\rangle$

$$|c_1^{(+\infty)}|^2 = |c_2^{(+\infty)}|^2 = 0, \tag{34}$$

$$|c_3^{(+\infty)}|^2 = \cos^2\left(\int_{-\infty}^{+\infty} \epsilon(t)dt\right), \tag{35}$$

$$|c_4^{(+\infty)}|^2 = \sin^2\left(\int_{-\infty}^{+\infty} \epsilon(t)dt\right). \tag{36}$$

Here the relation

$$\epsilon_1(t) = -\epsilon_2(t) =: -\epsilon(t), \quad \forall\, t \tag{37}$$

was used.[23]

Thus in the harmonic case, even for adiabatic evolution a superposition of the target states is eventually produced. Since the statistical weights of the two dressed states involved in the state vector are both equal in magnitude [see Eq. (28)] and hence at maximum, their behavior would consequently match with the foregoing analysis of the anharmonic system: The smaller Δ_h, the larger the contribution of a second dressed state. The dynamics of the harmonic system within the adiabatic approximation may so far be considered as a limiting case of an anharmonic system discussed previously. Figure 3 illustrates this behavior by depicting the contributions of dressed states $|1\rangle$ and $|2\rangle$ to the state vector at a characteristic time t^*.

However, as the harmonic system is more or less a "pathological" case of minor practical relevance, we shall henceforth concentrate on the anharmonic case.

2. Effects of permanent dipole moments

In deriving the expression for the RWA-Hamiltonian matrix, we have so far excluded the role of the diagonal elements of the dipole matrix μ_{jj}. The generalization of the RWA to N-level systems with nonvanishing μ_{jj} was derived by Nakai and Meath.[19] To this end they introduced an additional transformation of the form[24]

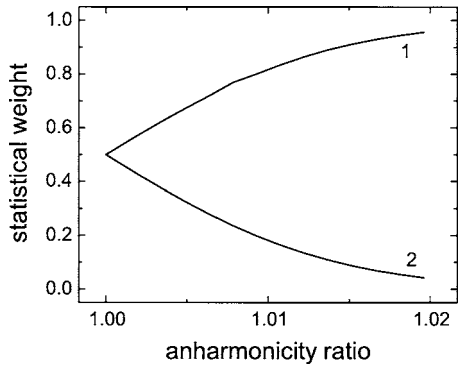

FIG. 3. Contribution of the instantaneous eigenvectors $|1\rangle$ and $|2\rangle$ to the RWA state vector $|\psi\rangle$ at (1+1)-on-resonance conditions as a function of the anharmonicity ratio f_h. Exemplarily shown are the statistical weights $|c_1|^2$ and $|c_2|^2$ at $t^*=15$ ps, where they display stationary behavior corresponding to the situation of both pulses present (compare Fig. 2). For $f_h=1$, both eigenstates contribute equally to $|\psi\rangle$. The driving pulse pair is the standard one from Table III.

$$\tilde{\mathbf{b}} := \mathbf{T}\mathbf{b},$$
$$T_{k,j} := e^{-i\gamma_k^\alpha}\delta_{k,j}, \tag{38}$$
$$\gamma_k^\alpha := \mu_{kk}E_\alpha\int_0^t \cos(\omega_\alpha s + \delta_\alpha)ds$$
$$= \frac{\mu_{kk}E_\alpha}{\omega_\alpha}(\sin(\omega_\alpha t + \delta_\alpha) - \sin\,\delta_\alpha),$$

to be subsequently applied on a vector $\mathbf{b}$, obtained by invoking the transformations included in the standard IR-RWA treatment. In Eq. (38), α has to be properly replaced by the pump pulse and Stokes pulse, respectively. The transformation accomplishes to eliminate the rapidly oscillating cosine terms in the diagonal elements of the original IR-Hamiltonian matrix, which afterwards are equal to those in the case when all μ_{jj} vanish, see Eq. (16).

The effects of nonzero μ_{jj} are consequently contained in the off-diagonal elements of the Hamiltonian matrix. They enter due to a characteristic parameter, z_{jk}^α, which is a measure for the relative strength of the permanent dipole moments considering the coupling $j \leftrightarrow k$, defined by

$$z_{jk}^\alpha := \frac{d_{jk}E_\alpha}{\omega_\alpha}, \quad d_{jk} := \mu_{jj} - \mu_{kk}. \tag{39}$$

After neglecting off-resonant and rapidly oscillatory terms analogous to the standard RWA, the off-diagonal elements $k > j$ finally read[19]

$$H_{j,k}^{\mathrm{RWA}} = -\tfrac{1}{2}E_\alpha\mu_{jk}e^{iz_{jk}^\alpha \sin\,\delta_\alpha}e^{i(k-j)\delta_\alpha}\{J_{k-j-1}(z_{jk}^\alpha) + J_{k-j+1}(z_{jk}^\alpha)\}, \tag{40}$$

which for $z_{jk}^\alpha \neq 0$ may be equivalently expressed as

$$H_{j,k}^{\mathrm{RWA}} = -E_\alpha\mu_{jk}e^{iz_{jk}^\alpha \sin\,\delta_\alpha}e^{i(k-j)\delta_\alpha}\frac{k-j}{z_{jk}^\alpha}J_{k-j}(z_{jk}^\alpha). \tag{41}$$

The remarkable point with Eq. (41) is that applied to our 4LS we also obtain a nonvanishing contribution of the *two-*

photon coupling μ_{24}. However, the strength of this term depends on the value of the Bessel function J_2 for given z_{jk}^{α}. More generally, the inclusion of permanent dipole moments μ_{jj} gives rise to additional coupling elements that are formally related to multiphoton processes,[25] where an n-photon term scales with a Bessel function of order n.

Furthermore, z_{jk}^{α} contains the driving field frequency ω_{α}. In particular, this means that the element $H_{1,2}$ of the Hamiltonian matrix will *explicitly* depend on ω_P, even though we have restricted our analysis to the on-resonance case Eq. (17).

Thus the inclusion of the effects of nonvanishing μ_{jj} gives rise to a dependence of the dynamics on ω_P, which we here represent as a dependence on f_{PS}, in addition to its dependence on Δ_h. This fact will become essential for the consideration of phase-dependent final populations, as this behavior was first found for certain ratios of pulse frequencies.[10]

The effects of nonvanishing μ_{jj} on the system's dynamics become clear, if we look at the characteristic equation that determines the dressed energies. In analogy to Eq. (18) for vanishing μ_{jj}, it becomes

$$0 = 16\lambda^4 + 16\lambda^3\Delta_h - 4\lambda^2\{E_S^2(\tilde{\mu}_{24}^2 + \tilde{\mu}_{23}^2 + \tilde{\mu}_{34}^2) + E_P^2\tilde{\mu}_{12}^2\} + 4\lambda\{E_S^2\tilde{\mu}_{23}\tilde{\mu}_{24}\tilde{\mu}_{34} - \Delta_h(E_S^2\tilde{\mu}_{23}^2 + E_P^2\tilde{\mu}_{12}^2)\} + E_P^2E_S^2\tilde{\mu}_{12}^2\tilde{\mu}_{34}^2. \quad (42)$$

Equation (42) is almost equivalent to the corresponding equation for no permanent dipole moment, Eq. (18), if the dipole matrix elements μ_{jk}, $j \neq k$, in Eq. (18) are replaced by the corresponding quantities $\tilde{\mu}_{jk}$ defined as

$$\tilde{\mu}_{jk} := \mu_{jk} 2(k-j)\frac{J_{k-j}(z_{jk}^{\alpha})}{z_{jk}^{\alpha}} \quad \text{for } z_{jk}^{\alpha} \neq 0. \quad (43)$$

However, due to the two-photon coupling that enters the RWA matrix, we also obtain additional terms in the characteristic polynomial Eq. (42). As will turn out, one of these two additional terms alters the dynamics in a essential way. To study its effects, we define the *splitting index* χ given by

$$\chi := E_S^3\tilde{\mu}_{23}\tilde{\mu}_{24}\mu_{34} - \Delta_h(E_S^2\tilde{\mu}_{23}^2 + E_P^2\tilde{\mu}_{12}^2), \quad (44)$$

where the leading term enters due to the inclusion of nonvanishing μ_{jj}. Note the dimension of χ is [energy^3]. We will henceforth make use of the same terminology as in the foregoing study of the dynamics without permanent dipole moment.

On IP, where only the Stokes field is present, there is still one eigenvalue ϵ_1 that equals zero. As we have shown for the case when all μ_{jj} are zero, the dynamics is determined by the "coupling" of the dressed states $|1\rangle$ and $|2\rangle$ corresponding to the eigenvalues ϵ_1 and ϵ_2, respectively, which evolve close to each other on IP.

Concentrating on the anharmonic case, the eigenstate $|1\rangle$ still corresponds to a transport state that leads from the initial state $|1_0\rangle$ to the target state $|3_0\rangle$. Possible diabatic transitions to state $|2\rangle$, which at the end of the interaction with the two laser fields coincides with target state $|4_0\rangle$,[26] are in accord with the necessary condition for adiabatic transport in nondegenerate systems, Eq. (5), determined by the splitting of the two related dressed energies ϵ_1 and ϵ_2.

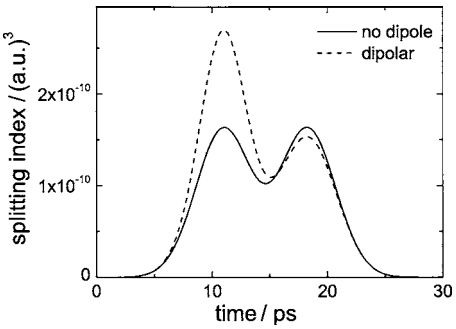

FIG. 4. Temporal behavior of the splitting index χ for the 3:2-4LS at (1+1)-on-resonance conditions. The parameters are the standard values from Table I, so that $f_h = 1.0590$. Solid line: standard RWA treatment without permanent dipole moments, $\mu_{jj}=0$; dashed line: dipolar system, μ_{jj} from Table II. The driving pulse pair is the standard one from Table III.

In order to make assertions about this splitting we consider a time interval which we designate *extended* IP (EIP).

Extended IP (EIP): The Stokes field interacts with the system

$$E_S \neq 0. \quad (45)$$

The pump field has already started to act; however, it is assumed to be "small" enough to fulfill

$$E_P^2E_S^2\tilde{\mu}_{12}^2\tilde{\mu}_{24}^2 \approx 0. \quad (46)$$

Obviously, this time interval contains IP; however, it is extended to times where one can assume the term $E_P^2E_S^2\tilde{\mu}_{12}^2\tilde{\mu}_{34}^2$ to be negligible, as it is of order $\mathcal{O}(E_{\alpha,0}^4)$. After reduction of the characteristic polynomial of Eq. (42), by one order of λ, corresponding to $\epsilon_1=0$, the remaining polynomial within the EIP reads

$$\tilde{p}(\lambda) := 16\lambda^3 + 16\lambda^2\Delta_h - 4\lambda\{E_S^2(\tilde{\mu}_{24}^2 + \tilde{\mu}_{23}^2 + \tilde{\mu}_{34}^2)E_P^2\tilde{\mu}_{12}^2\} + 4\chi. \quad (47)$$

From this equation the meaning of χ as well as the reason for choosing the name "splitting index" becomes evident. Thus the temporal behavior of χ determines the splitting of the eigenvalues ϵ_1 and ϵ_2, respectively, which become degenerate, $\epsilon_1=\epsilon_2=0$, for $\chi=0$.

However, as in χ the additional term

$$\eta := E_S^3\tilde{\mu}_{23}\tilde{\mu}_{24}\tilde{\mu}_{34} \quad (48)$$

arises, if the effects of permanent dipole moment are included in the theory, its temporal behavior will be different compared to the RWA analysis, where these effects have been excluded. Figure 4 compares χ as a function of time for the two cases, *with* and *without* the inclusion of permanent dipole moment.

From Fig. 4 it follows that the additional term in χ strongly alters its behavior on EIP, giving rise to a thoroughly pronounced maximum in this time interval. This essential change of χ related to the formal inclusion of μ_{24} consequently affects the dressed energies ϵ_1 and ϵ_2. Numerical solution of the characteristic equation shows that it leads,

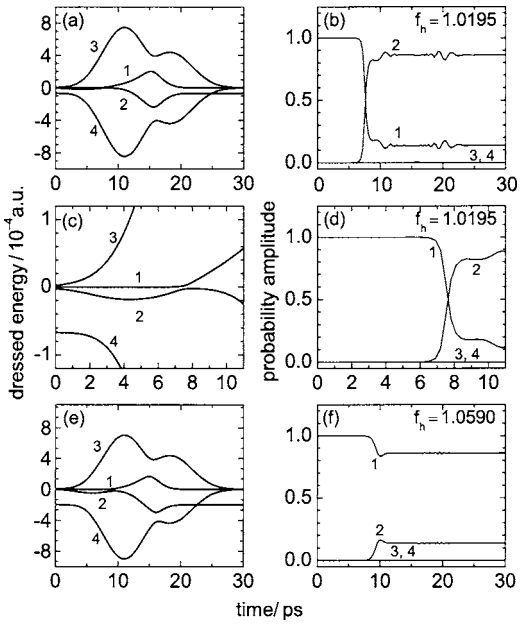

FIG. 5. Effects of permanent dipole moments on the RWA dressed states and the state vector. Panels (a), (b), (e), and (f) are exact counterparts of the dipole-free cases in panels (c)–(f) of Fig. 2. As a consequence of the inclusion of the dipole moment, an avoided crossing arises between $|1\rangle$ and $|2\rangle$ that leads to strong coupling and diabatic transitions between these states. Panels (c) and (d) zoom into the extended initial period of panels (a) and (b) to highlight this dipole-induced avoided crossing. A comparison of panels (b) and (f) shows that the influence of the avoided crossing on the dynamics decreases with increasing anharmonicity.

in fact, to the development of an avoided crossing between these two eigenvalues. This is demonstrated in Fig. 5 for the case of the 3:2-4LS.

As a consequence of Eq. (5), this avoided crossing leads to strongly pronounced diabatic transitions between the dressed states $|1\rangle$ and $|2\rangle$. As Δ_h does not enter η, which gives rise to the avoided crossing, this effect will be weakened with increasing Δ_h (or f_h), as was the case with the system with no permanent dipole moment.

B. Phase-dependent final populations

Having analyzed the dynamics of our extended Λ system in considerable detail, we are now able to turn to the question of phase-dependent final populations of the target states $|3_0\rangle$ and $|4_0\rangle$. Since diabatic transitions are controlled by the parameters Δ_h and ω_P that finally lead to populations of *both* target states, phase dependence can only arise if the transition probability for the diabatic coupling between the two dressed states $|1\rangle$ and $|2\rangle$ becomes phase dependent. Furthermore, the parameters given above, which control these transitions, should also control phase-dependent behavior. Hence, we have to investigate the dressed energies as well as the dressed states for an additional dependence on δ.

We first consider the dressed energies. Including $\mu_{jj} \neq 0$, we have to solve for the roots of the characteristic equation of the Hamiltonian matrix with elements given as in Eq. (41), where

$$\delta_\alpha = \begin{cases} \delta \in [0, 2\pi] & \text{for } \alpha = P \\ 0 & \text{for } \alpha = S. \end{cases} \tag{49}$$

To this end, we consider the characteristic equation

$$0 \overset{!}{=} \det(\underbrace{\mathbf{H} - \lambda \mathbf{I}_4}_{=:\mathbf{A}}), \tag{50}$$

where the Hermitian matrix $\mathbf{A}$ assumes the form

$$\mathbf{A} = \begin{pmatrix} A_{1,1} & A_{1,2} & 0 & 0 \\ \overline{A_{1,2}} & A_{2,2} & A_{2,3} & A_{2,4} \\ 0 & \overline{A_{2,3}} & A_{3,3} & A_{3,4} \\ 0 & \overline{A_{2,4}} & \overline{A_{3,4}} & A_{4,4} \end{pmatrix} \quad \text{with } A_{j,j} \in \mathbb{R}. \tag{51}$$

Expansion with respect to the first row yields

$$\det(\mathbf{A}) = A_{1,1} \cdot S_{1,1} - A_{1,2} \cdot S_{1,2},$$

$$S_{1,1} := A_{2,2}A_{3,3}A_{4,4} + 2\,\mathrm{Re}(A_{2,3}A_{3,4}\overline{A_{2,4}}) - |A_{2,4}|^2 A_{3,3} - |A_{3,4}|^2 A_{2,2} - |A_{2,3}|^2 A_{4,4},$$

$$S_{1,2} := \overline{A_{1,2}}(A_{3,3}A_{4,4} - |A_{3,4}|^2).$$

As the phase only enters the coupling element $H_{1,2}$

$$H_{1,2} = -\tfrac{1}{2}\tilde{\mu}_{12}E_P \exp\{i(\delta + z_{12}^P \sin\delta)\}, \tag{52}$$

and the determinant of $\mathbf{A}$ solely contains the absolute squared norm of this element, the characteristic polynomial is independent of δ and hence so are its roots.

The characteristic features of the dynamics, as given by the temporal behavior of the dressed energies, are therefore shown to be *independent* of phase. Whether a phase dependence in the final populations is given within the RWA, now lies completely in the dressed states. Again, as a closed form of the dressed states will be rather unwieldy, we will restrict the further analysis to results of numerical calculations by solving the time-dependent RWA-Schrödinger equation, and considering whether a phase dependence of its solution arises for $t \to +\infty$. If so, the dressed states $|1\rangle$ and $|2\rangle$ are bound to bear a phase dependence that is not physically trivial, i.e., does not vanish when the physically relevant absolute squares of the components are considered.

First, we consider the 3:2-4LS. As the inclusion of the permanent dipole moment significantly changes the dynamics, we will compare results for our standard pulse setting for the two cases *with* and *without* taking into account the effects of nonvanishing μ_{jj}. While for the nonpolar system, we find $|c_3|^2 = 1$ and $|c_4|^2 = 0$ independent of δ, in the dipolar system the population varies from 0.856 to 0.865 for target state $|3_0\rangle$, and correspondingly from 0.144 to 0.135 for state $|4_0\rangle$. Hence, only the inclusion of permanent dipole moments leads to a phase dependence in the final populations for the 3:2-4LS. In this case, the dressed states $|1\rangle$ and $|2\rangle$ bear a phase dependence that is physically nontrivial.

For further analysis we define the overall phase sensitivity ϕ_j of the state $|j_0\rangle$ as

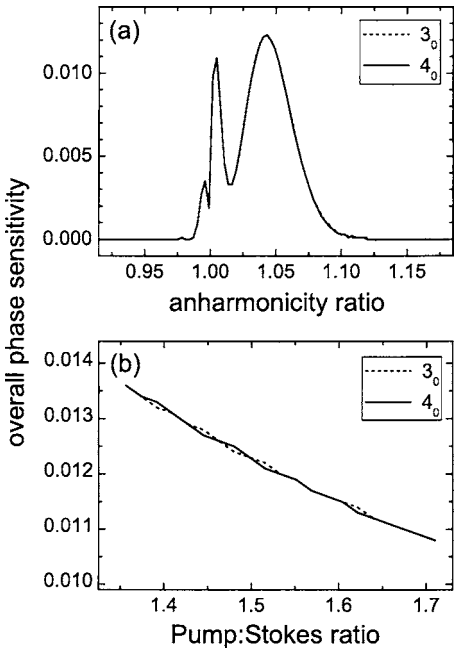

FIG. 6. Overall phase sensitivities ϕ_3 and ϕ_4 from a RWA analysis, obtained for the 3:2-4LS at (1+1)-on-resonance conditions. Panel (a): Dependence of ϕ_3 and ϕ_4 on the anharmonicity ratio f_h. Note that ϕ_3 and ϕ_4 coincide on the interval considered, their maximum appearing at $f_h=1.0433$, while ϕ_1 and ϕ_2 are negligibly small. Panel (b): Dependence of ϕ_3 and ϕ_4 on the pump:Stokes ratio f_{PS} for (1+1)-on-resonance conditions. The anharmonicity ratio f_h is set to 1.0433, corresponding to the maximum of panel (a). Weak oscillations in ϕ_3 and ϕ_4 indicate minute perturbations of STIRAP-like transport as ω_P is varied. Again ϕ_1 and ϕ_2 are negligibly small.

$$\phi_j := \lim_{t\to+\infty}\left\{\max_{\delta\in[0,2\pi]}|c_j(t;\delta)|^2 - \min_{\delta\in[0,2\pi]}|c_j(t;\delta)|^2\right\}, \tag{53}$$

where we expect the relations

$$\phi_3 = \phi_4, \quad \phi_1 = \phi_2 = 0 \tag{54}$$

to hold for STIRAP-like transport processes. In such cases we will sometimes drop the explicit reference to the state and simply speak of the overall phase sensitivity ϕ.

It now remains to identify the parameters that control the ϕ_j. Since only those parameters that influence the dynamics in the case $\delta=0$ are possible candidates, we have to consider the effects of variations of f_h and f_{PS}, which are illustrated in Fig. 6.

We start with discussing the dependence on Δ_h. For zero permanent dipole moment, we find no phase-dependent behavior of the final populations. However, panel (a) in Fig. 6 shows that for nonzero μ_{jj} a nonzero overall phase sensitivity is observed, and ϕ_3 and ϕ_4 exhibit a common global maximum at $f_h=1.0433$. The decrease of ϕ for larger values of f_h can be understood as a consequence of the increasing eigenvalue splitting according to Eq. (44).

We next address the influence of f_{PS}, which we vary at fixed anharmonicity. In panel (b) of Fig. 6, we show the ϕ_j as a function of f_{PS} with f_h fixed at=1.0433, corresponding to the value of maximum phase sensitivity in the 3:2-4LS. In accord with the starting point of our work,[10] the plot shows that ϕ_3 and ϕ_4 depend on f_{PS}.

Summing up, phase-dependent final populations in an extended Λ system as discussed here may hence be explained within the framework of the RWA. They arise as a result of explicitly incorporating permanent dipole moments, which formally leads to a contribution of the nonzero two-photon coupling related to μ_{24}. Thus we may interpret phase-dependent behavior as a result of *both* nonzero two-photon coupling of the spectroscopic states $|2_0\rangle \leftrightarrow |4_0\rangle$ and of permanent dipole moments μ_{jj}. However, this last interpretation has to be verified by simulations that are correctly incorporating direct multiphoton processes. In order to complete our analysis, we will now compare the conclusions drawn from the treatment within the RWA with results obtained by a direct numerical integration of the Schrödinger equation.

IV. RESULTS FROM A FULL NUMERICAL TREATMENT

In this section we present results on the dynamics of the 4LS obtained by direct numerical propagation without making any approximations in the semiclassical Hamiltonian Eq. (2). This, in particular, means that we do not invoke the coupling approximation, introduced in Sec. II B for the coupling of the field to the individual level pairs of the system. In Sec. IV A we first consider (1+1)-on-resonance conditions paralleling the RWA analysis in the previous section. In addition in Sec. IV B we investigate separately the effects of permanent dipole moments and of direct overtone coupling. In Sec. IV C we extend the investigation to off-resonance conditions. This allows us to to find the maximum phase sensitivity, to draw conclusions concerning the robustness of STIRAP under conditions of phase sensitivity, and to identify the signatures of phase-sensitive behavior in ω_P-ω_S space. The standard parameters of the Gaussian pulses we are using in these simulations are those shown in Table III.

A. Comparison with the RWA analysis

In the RWA treatment we find that for fixed field strength the ϕ_j are controlled by f_h and f_{PS}. Corresponding results for the dependence of the phase sensitivity on these two parameters from the full numerical treatment are shown in Fig. 7. For a variation of f_h in the 3:2-4LS, ϕ_3 and ϕ_4 are found to be more than one order of magnitude more pronounced than in the RWA (see Fig. 6). Qualitatively though, there are clear similarities to the behavior obtained within the RWA. As there, ϕ exhibits a global maximum. Comparison of Fig. 6(a) and Fig. 7(a) shows that, in fact, the agreement is fair only for relatively small anharmonicities $f_h \leqslant 1.06$. For larger values of f_h the full simulations predict sizable phase effects, while the RWA results do not. However, this latter behavior is not unexpected: since in the RWA only quasiresonant terms are retained within the IR Hamiltonian, this puts a limit on the value of f_h to be considered within its range of validity.

As for the dependence of ϕ_j on f_{PS}, we consider its variation in a system with $f_h=1.0963$ a.u., corresponding to the previously detected maximum of phase sensitivity for the 3:2-4LS. In order to achieve STIRAP-like behavior, in particular, to guarantee sufficiently distinct pump and Stokes frequencies,[27] ω_P is varied in the range of 1.32–1.73. In Fig. 7 we detect a complex oscillatory behavior with a number of

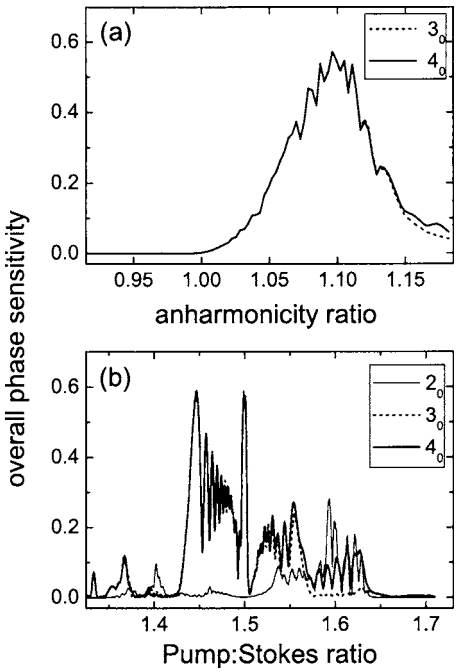

FIG. 7. Overall phase sensitivities ϕ_2, ϕ_3, and ϕ_4 from a numerical treatment of the full Hamiltonian, obtained for the 3:2-4LS at $(1+1)$-on-resonance conditions. The plots complement the RWA analysis in Fig. 6. Panel (a): Dependence of ϕ_3 and ϕ_4 on the anharmonicity ratio f_h. ϕ_3 and ϕ_4 are closely coincident on the interval considered, their maximum appearing at $f_h=1.0963$, while ϕ_3 and ϕ_4 are negligibly small. Panel (b): Dependence of ϕ_2, ϕ_3, and ϕ_4 on the pump:Stokes ratio f_{PS} for $(1+1)$-on-resonance conditions. Here f_h is set to 1.0963, corresponding to the maximum of panel (a). The plot is obtained from 1000 grid points, the fast oscillations near $f_{\mathrm{PS}}=1.45$ are not fully resolved. For $f_{\mathrm{PS}}\geqslant 1.56$ ϕ_3 and ϕ_4 do not coincide due to deviations from STIRAP-like transport; there are also weak frequency-dependent perturbations for smaller values of f_{PS} manifest as $\phi_2\neq 0$, indicating residual phase-dependent population in the apex state $|2_0\rangle$.

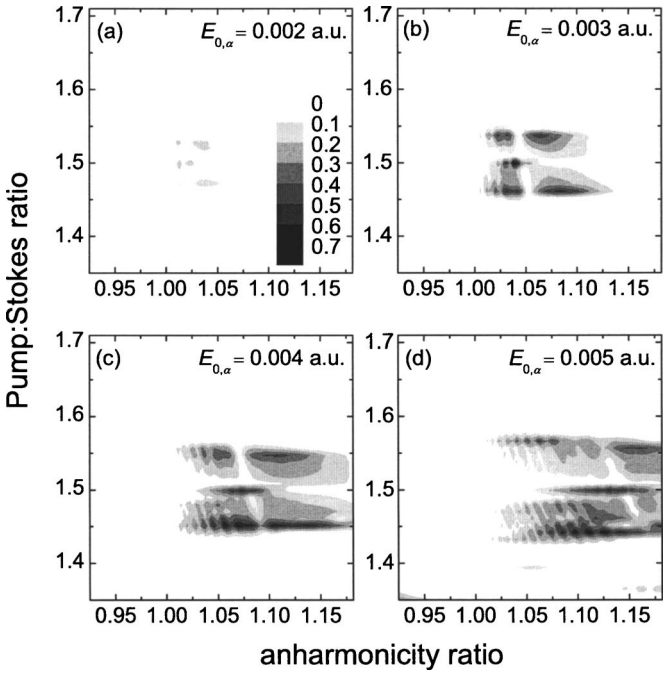

FIG. 8. Simultaneous dependence of the overall phase-sensitivity ϕ_3 on the anharmonicity ratio f_h and the pump:Stokes ratio f_{PS} from a numerical treatment of the full Hamiltonian, obtained for $(1+1)$-on-resonance conditions. Panels (a)–(d): Contour plots for various field strengths $E_{0,\alpha}$ as indicated. The common scale for the plots is included in panel (a).

local maxima and minima. Although one of the maxima corresponds to a frequency ratio $\omega_P/\omega_S=3/2$ resembling the findings in Ref. 10, there are other local maxima on the interval considered which cannot be related to any simple commensurable frequencies. Whereas we could explain the role of f_{PS} (and hence implicitly of ω_P) for phase-dependent final populations within the RWA, the detailed behavior of ϕ vs ω_P, exhibiting local maxima and minima corresponding to partial amplifications and extinctions, cannot be explained within the limitations of this theory.

The contour plots in Fig. 8 show that the trends in both one-dimensional cuts in Fig. 7 are typical ones and are not compromised by the specific choice of conditions. In the ranges where phase sensitivity does appear, ϕ shows oscillatory behavior both with respect to variations in f_h and f_{PS}, clearly indicative of interference effects. We also see that moderately increasing the field strength $E_{0,\alpha}$ increases the amount of phase sensitivity and extends the range of frequencies where it can be observed, but again the overall behavior is left unchanged. Note in our simulations we have ascertained that the values of $E_{0,\alpha}$ are sufficiently large to guarantee adiabatic transport in the time range where the two pulses overlap strongly.

In summary it appears that within predictable limits the conclusions drawn from the RWA treatment are in accord with the results from a numerical integration of the Schrödinger equation. Definitely, the degree of the phase sensitivity obtained in the fully numerical calculations is much more enhanced than the corresponding effects in the RWA. This may be related to the fact that phase dependence has been shown to be a consequence of both the nonzero two-photon coupling as well as the permanent dipole moment. Although the two-photon coupling formally enters the RWA when including nonvanishing μ_{jj}, its strength given by μ_{24} is considerably diminished by a prefactor containing the Bessel function of second order [see Eq. (43)]. On the other hand, invoking the RWA also means accepting an upper bound with respect to the field strength, since it demands[14]

$$|\mu_{kj}E_{0,\alpha}| \ll \omega_\alpha, \tag{55}$$

to hold for the coupling element $H_{k,j}$, $k\neq j$. Hence in connection with the conditions on $E_{0,\alpha}$ posed in order to guarantee sufficiently adiabatic evolution of the system, in general there may arise difficulties with the overlap of the range of validity of the adiabatic approximation on the one hand and the RWA on the other.

B. Elements of the phase sensitivity

Following the arguments of Sec. III B, we have interpreted phase-dependent behavior as a result of the interplay of two factors: the nonzero two-photon coupling related to $\mu_{24}=0$ and the nonvanishing μ_{jj}. As these effects are coupled within the RWA, we have not been able to discuss them separately. On the basis of the simulations using the full Hamiltonian we can attempt to disentangle some of the effects. In order to do so, we modify our basic Hamiltonian

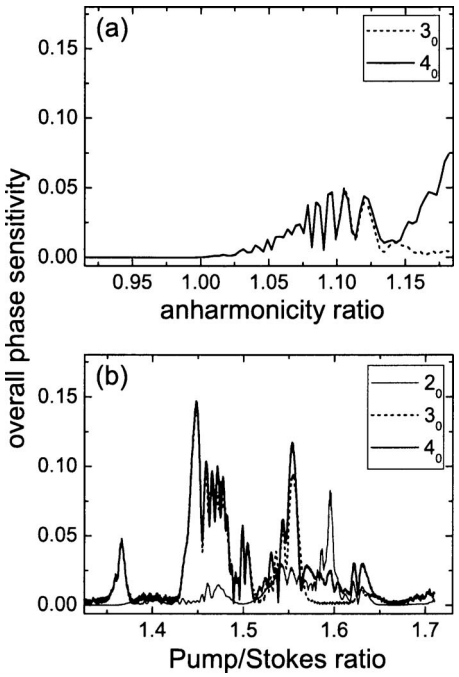

FIG. 9. As Fig. 7, but with the overtone coupling μ_{24} set to zero.

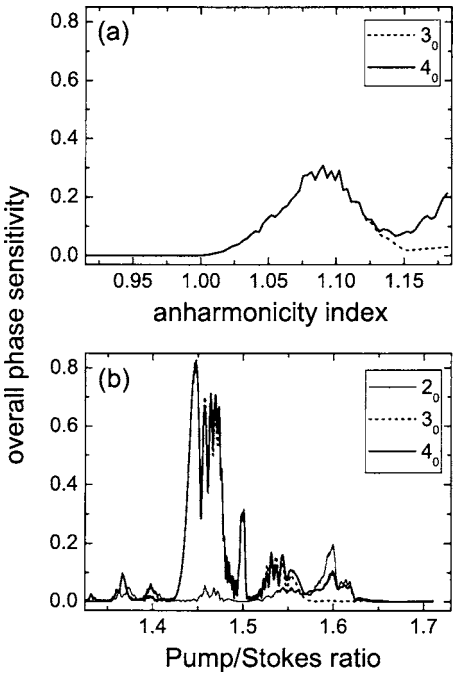

FIG. 10. As Fig. 7, but with the dipole moments μ_{jj} set to zero.

and suppress in turn separately μ_{24} and μ_{jj} (and both). We start with the investigation of the influence of μ_{jj} by setting $\mu_{24}=0$. This situation corresponds to a hypothetical purely sequential 4LS with permanent dipole moments. Figure 9 depicts the corresponding results. Phase-dependent behavior of the final populations is still observed in the sequentially coupled dipolar system, although the suppression of direct two-photon coupling reduces ϕ by about an order of magnitude.

Investigating now the role of the two-photon coupling related to μ_{24} in isolation, we consider a nonpolar system by assuming $\mu_{jj}=0$, $1\leqslant j\leqslant 4$. The results of the corresponding simulations are illustrated in Fig. 10. Again the most important observation is that phase sensitivity is still present in the nonpolar system, which means this behavior can be induced by direct overtone coupling irrespective of its origin. In more detail, the reduced dependence of ϕ on f_h seen in panel (a) as compared with the corresponding results for the full dipolar Hamiltonian in Fig. 7 could be understood on the basis of the RWA analysis, where we have shown that the inclusion of permanent dipole moments leads to much stronger diabatic coupling and therefore the possibility of enhanced phase effects. The results in panel (b), which suggest a partial increase of the phase sensitivity in the nonpolar system relative to the full dipolar one, cannot be understood on the basis of the analysis within the RWA, although based on more extended results of the full simulations, we will address this problem in a heuristic interpretation in terms of interference effects.

So far the discussion suggests that the phenomenon of phase-sensitive final populations is caused both by the nonzero permanent dipole moments as well as by the existing two-photon coupling related to μ_{24}, and that it would also exist for nonpolar systems with sufficiently strong overtone coupling. The overall effect for the full system bearing both these characteristic features then must result from a superposition of the individual effects, which would be sensitive to interference. At this point we note that for a system, which includes neither the direct two-photon coupling $|2_0\rangle \leftrightarrow |4_0\rangle$ nor nonzero μ_{jj}, we find no phase-dependent behavior whatsoever.

The results from the full simulations suggest a heuristic interpretation of phase-sensitive behavior as arising from a two- (or more-) path situation, where the target states are accessible by different mechanisms, either sequentially or via multiphoton-overtone transitions. Interference effects associated with this situation will give rise to an oscillatory behavior of ϕ as observed, in particular, with respect to its dependence on f_{ps}. The observed decrease of ϕ for the full system as compared with the nonpolar one then has an explanation as an interference effect, which (fortuitously) happens to be weakly destructive at the specific conditions in question. Indeed we find that the relative magnitudes of ϕ for the three cases (full Hamiltonian versus $\mu_{jj}=0$ vs $\mu_{24}=0$) can be totally different for different frequency combinations away from the $(1+1)$-on-resonance case.

C. Off-resonant frequencies: Robustness and the signatures of phase sensitivity

In order to explore the full extent of phase sensitivity, we now extend our simulations to off-resonant frequencies. Contrary to the previous sections, this means that ω_P and ω_S are used to explore the full frequency scale and are no longer fixed to the $(1+1)$ zero-order resonance values. We keep the system parameters fixed as those of the 3:2-4LS with $f_h=1.0963$, which is a case that gave a particularly large value of ϕ for the $(1+1)$-on-resonance situation.

These simulations will reveal how robust the transfer remains if phase sensitivity arises in a STIRAP-like setup. In Fig. 11 we present contour plots of final target populations in

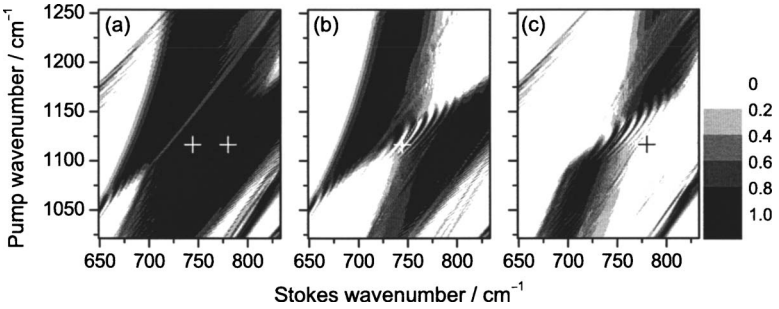

FIG. 11. Contour plots of the final target populations in the 3:2-4LS with $f_h=1.0963$ (this value maximizes the phase sensitivity; see also Fig. 7), standard pulse parameters, phase $\delta=0$. Panel (a): Total target population from (1+1) and (1+2) processes. The crosses mark the (1+1)- and (1+2)-on-resonance frequencies. Panel (b): (1+1)-STIRAP to target state $|3_0\rangle$; the cross marks the (1+1)-on-resonance frequencies. Panel (c): (1+2)-STIRAP to target state $|4_0\rangle$; the cross marks the (1+2)-on-resonance frequencies.

the (ω_P, ω_S) plane for the phase fixed as $\delta=0$. Panels (a)–(c) show in turn the total transfer probability, i.e., the sum of the (1+1)- and (1+2)-transfer probabilities, relating to the robustness of the overall transfer process, and the two individual contributions, indicating the properties of target state branching. Note in these plots we adopt a wave number representation in order to emphasize the extent of robustness in an experimental context. The remarkably large range of complete or near complete population transfer to the "products" shows that the usual robustness of (1+1)-STIRAP still prevails, and suggests STIRAP could be a useful technique for molecular isomerization reactions (see Ref. 20 for a similar conclusion). We find that contour plots for different fixed values of δ have the same appearance, indicating that the assumption $\phi_3=\phi_4$ is valid over the entire range spanned by the plot, so that it is just the product branching ratio that is affected by any phase sensitivity.

This latter point is more clearly seen in panels (b) and (c) of Fig. 11, which demonstrate that the range of robust (1+1) transfer is the more extended one. Most intriguingly, however, there is a range of balanced rapidly oscillatory change of the populations near the center of the two plots, which is the signature of phase sensitivity in a situation without phase variation. For both plots we have $\delta=0$ (and similar, but clearly shifted patterns are obtained for different fixed values of δ). Locally (in time) for a field obtained by superposition of two pulses with different frequencies, a slight change of one of the frequencies has an effect similar to a slight variation of its phase, so that in the range of phase sensitivity, frequency variation in some sense emulates phase variation. We also observe transitional ranges where the phase dependence is weak, so that target superpositions with "phase-stable" branching ratio are formed.

The oscillatory effect in the phase-sensitive range is more dramatically demonstrated in Fig. 12, where we zoom into the oscillatory range around the (1+1)-on-resonance frequencies change, for demonstration purposes only, to $\delta=\pi/8$, and superimpose the populations of the target states $|3_0\rangle$ and $|4_0\rangle$ such that each of the two colors (gray versus black) corresponds to a population of more than 50% in one of the states (noting also that the total transfer probability is close to 100% throughout this range). The oscillations are the clear signatures of phase sensitivity in a setup without phase variation. The (1+1)-on-resonance case, serving as our reference in the RWA investigations, lies well within the sensible range. We note that the phase effects may be even

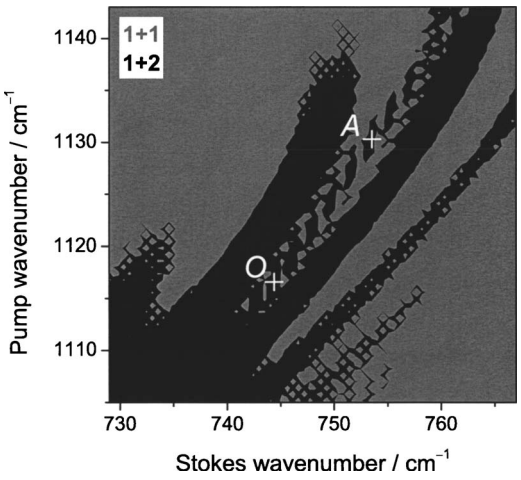

FIG. 12. Contour plot with the individual target populations of the (1+1) and (1+2) processes superimposed. System and pulse parameters are as in Fig. 11, except that we zoom into the central frequency range and set the phase at $\delta=\pi/8$. Gray areas: (1+1)-STIRAP dominates, >50% population in $|3_0\rangle$; black areas: (1+2)-STIRAP dominates, >50% population in $|4_0\rangle$. The strong frequency-dependent oscillations indicate the phase sensitivity of the target populations. The points marked O and A denote, respectively, the (1+1)-on-resonance frequencies and the point of maximum phase sensitivity (see Fig. 13).

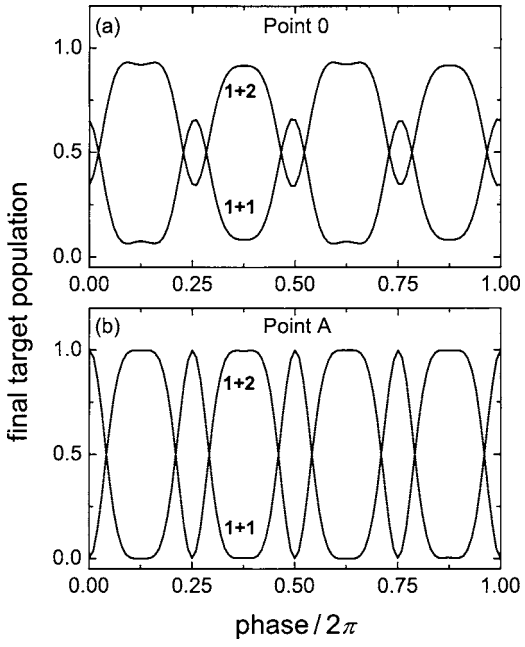

FIG. 13. Explicit phase dependence of target state populations for selected frequency pairs from Fig. 12. Panel (a): On resonance case, point O of Fig. 12. Panel (b): Complete phase-dependent target level switching is observed at slightly off-resonant conditions, point A of Fig. 12.

larger in certain off-resonant situations, indicated by an even more pronounced oscillatory character of the target populations. Indeed at the point marked A we find that the phase sensitivity assumes its maximum $\phi=1$, so that upon variation of δ the populations of the target states oscillate between 0 and 1. In Fig. 13 we show the explicit phase dependence at the on-resonance point O, where ϕ is about 60%, and at point A with its complete phase-induced level switching.

V. SUMMARY AND CONCLUSIONS

In this paper we provide means for understanding the role of the relative phase in STIRAP-like transport processes in a molecular extended Λ system. To this end we use a dressed state representation within the RWA to display the system's dynamics. This adiabatic approach proved to be more advantageous than a perturbative treatment of the dynamics,[16] which up to third order shows no phase dependence in the populations. Furthermore, we augment the analytical treatment with numerical simulations using the full semiclassical Hamiltonian without any further approximations.

In the RWA treatment we find that only two of the dressed states contribute to the state vector, each coinciding finally with *one* of the two target states. The mechanism for creating a certain superposition of the target states can thus be identified with nonadiabatic coupling among these two dressed states. In particular, phase sensitivity of the target state branching has been shown to arise as a result of phase-dependent diabatic transitions controlled by the anharmonicity of the energy level structure on the target side, the pump:Stokes ratio and the field strength.

However, this dependence of diabatic coupling on the relative phase only arises if (different) nonzero diagonal elements of the dipole matrix are included. As this inclusion formally leads to an additional two-photon coupling in connection with the nonzero dipole matrix element μ_{24}, we interpret phase-dependent behavior as a consequence of *both* nonzero two-photon coupling of the states $|2_0\rangle \leftrightarrow |4_0\rangle$ and of *differences* in the permanent dipole moments of the initial, intermediate, and target states.

Comparing the RWA results with those from numerical simulations, we find that the implications of the analytical treatment can be carried over to the full Hamiltonian. Although the phase sensitivity detected in these computer simulations turns out to be considerably stronger, and to cover a distinctly larger region in parameter space, the qualitative behavior as well as the effects obtained in these calculations are in accord with the conclusions drawn from the RWA treatment. The observed deviations and, in particular, the limits of validity of these comparisons can be understood on the basis of the simplifications and additional approximations inherent in the RWA. The more extended scope of the numerical simulations permits a heuristic interpretation of the phase effects on a different level of phenomenology, namely, as arising from interferences in a two-path situation, where the lower target state can be accessed either sequentially or via direct overtone coupling (which may be dipole assisted).

We have thus shown that this novel phenomenon of phase sensitivity in STIRAP-like transport processes taking place in systems relevant, e.g., for the study of chemical reactions arises as a consequence of fundamental properties of general molecular systems such as permanent dipole moment and direct n-photon couplings, i.e., by admitting systems that do not obey the strict symmetry rules of the standard STIRAP ansatz. We have also been able to qualitatively understand important aspects of these processes on the basis of an analysis carried out within the RWA.

ACKNOWLEDGMENTS

The authors thank Shaul Mukamel for valuable comments. This work was supported by the Austrian Science fund within the framework of the Special Research Program F016 "ADLIS."

[1] U. Gaubatz, P. Rudecki, S. Schiemann, and K. Bergmann, J. Chem. Phys. **92**, 5363 (1990).
[2] G. W. Coulston and K. Bergmann, J. Chem. Phys. **96**, 3467 (1991).
[3] M. P. Fewell, B. W. Shore, and K. Bergmann, Aust. J. Phys. **50**, 281 (1997).
[4] B. W. Shore, K. Bergmann, J. Oreg, and S. Rosenwaks, Phys. Rev. A **44**, 7442 (1991).
[5] N. V. Vitanov, B. W. Shore, and K. Bergmann, Eur. Phys. J. D **4**, 15 (1998).
[6] N. V. Vitanov, Phys. Rev. A **58**, 2295 (1998).
[7] B. W. Shore, K. Bergmann, A. Kuhn, S. Schiemann, and J. Oreg, Phys. Rev. A **45**, 5297 (1992).
[8] J. Gong and S. A. Rice, Phys. Rev. A **69**, 063410 (2004).
[9] A. Karpati and Z. Kis, J. Phys. B **36**, 905 (2003).
[10] I. Vrábel and W. Jakubetz, J. Chem. Phys. **118**, 7366 (2003).
[11] B. H. Bransden and C. J. Joachain, *Physics of Atoms and Molecules* (Longman, London, 1983).
[12] K. Bergmann, H. Theuer, and B. W. Shore, Rev. Mod. Phys. **70**, 1003 (1998).
[13] M. Elk, Phys. Rev. A **52**, 4017 (1995).
[14] M. Quack, Adv. Chem. Phys. **1**, 395 (1990).
[15] K. B. Whaley and J. C. Light, Phys. Rev. A **29**, 1188 (1983).
[16] A. Messiah, *Quantenmechanik Band 2* (Walter de Gruyter, Berlin, 1990).
[17] M. Quack and E. Sutcliffe, J. Chem. Phys. **83**, 3805 (1985).
[18] J. Oreg, K. Bergmann, B. W. Shore, and S. Rosenwaks, Phys. Rev. A **45**, 4888 (1992).
[19] S. Nakai and W. J. Meath, J. Chem. Phys. **96**, 4991 (1992).
[20] V. Kurkal and S. A. Rice, Chem. Phys. Lett. **344**, 125 (2001).
[21] J. M. Bowman, B. Gazdy, J. A. Bentley, T. J. Lee, and C. E. Dateo, J. Chem. Phys. **99**, 308 (1983).
[22] W. Jakubetz and B.-L. Lan, Chem. Phys. **217**, 375 (1997).
[23] This follows readily from the symmetry of the characteristic polynomial Eq. (18) for $\Delta_h=0$.
[24] In order to keep our development as compact as possible, we include the relative phase in the general equations [Eqs. (38)–(41)], though we shall explicitly refer to and discuss its role not until Sec. III B.
[25] Still, direct multiphoton processes, i.e., transfer processes that do not require quasiresonant intermediate states, cannot be treated correctly in this more general RWA (Ref. 19).
[26] As the additional coupling element is associated with the two-photon coupling term $H_{2,4}$, which is assumed to be related to the Stokes pulse only, the results for the eigensystem on FP [see Eq. (27)] are not altered by the introduction of nonzero dipole matrix elements μ_{jj}. Only the matrix elements μ_{jk}, $k \neq j$ have to be replaced by the corresponding elements $\tilde{\mu}_{jk}$, Eq. (43).
[27] This ensures that the pump pulse does not act as Stokes pulse or vice versa.